Indentation Loading of Prismatic Cell Lithium-ion Battery Modules

Sida Xu[1] and David Sypeck[2]
Embry-Riddle Aeronautical University, Daytona Beach, FL, 32114, USA

Li-ion batteries are widely used as electric power sources for smartphones, tablets, laptops, unmanned aerial vehicles, e-scooters, electric vehicles, and numerous other transportable electronic devices. Li-ion battery modules with prismatic cells were subjected to destructive quasi-static indentation using a V-shaped stainless steel wedge indenter to investigate the effects of different loading orientation and direction. The modules were discharged to a very low state of charge for testing. Force and voltage were then measured as a function of displacement to monitor the damaging effects of indentation on electrical performance. Progression of damage of the cells within the modules was photographed and documented. Results differed substantially depending on loading orientation and direction. In many cases, voltage dropped quickly as the wedge damaged the cells. This research will help engineers expand their knowledge on the effects of various loading to high-voltage battery modules.

I. Nomenclature

APU = auxiliary power unit
EV = electric vehicle
LIB = lithium-ion battery
SOC = state of charge

II. Introduction

With the current climate of internal combustion engine powered vehicles transitioning to electric vehicles (EVs), the use of lithium-ion batteries (LIBs) has become an increasingly important topic of investigation. These types of batteries are widely used as electric power sources for smartphones, tablets, laptops, unmanned aerial vehicles, e-scooters, and numerous other transportable electronic devices. They are also popular in the aerospace industry, where for example, some Cessna (Wichita, KS) Caravan and Bombardier (Montreal, Québec, Canada) Dash-8 aircraft use small LIBs as their main battery [1]. Similarly, the Boeing (Chicago, IL) 787 uses a LIB for its auxiliary power unit (APU) [2]. Airport equipment and vehicles are also electrifying [3], and some next generation electric aircraft are using LIBs as their main power source [4]. However, the pace of adoption has been slower than envisioned, in part due to performance issues, safety concerns, and public apprehension.

When batteries are excessively loaded, damage can occur. Xia et al. [5] observed the mechanical, electrical, and thermal responses of impact damaged pouch cell LIB modules using various types of indenters and state of charge (SOC). In another study, Kalnaus et al. [6] indented stacks of lithium-ion pouch cells at various speeds after placing them in a specially designed enclosure representative of a battery module. Zhu et al. [7] used a stainless steel V-shaped wedge to quasi-statically load a pouch cell battery module and study module level damage under large plastic deformation. More recently, prismatic LIB cells and modules were indented while monitoring voltage to investigate the effect of damage on electrical performance [8, 9]. Here, the module indentation experiments are extended to include additional indentation orientations and observations. A total of six quasi-static experiments are used to show the effects of different loading orientation and direction on indentation force and battery voltage as a function of actuator displacement. Another higher rate test is included to investigate the strain rate effect. Progression of damage of the cells within the modules was photographed and documented.

[1] Graduate Student, Department of Aerospace Engineering, AIAA Student Member.
[2] Professor, Department of Aerospace Engineering.

III. Experimental

The modules consist of six prismatic cells connected in series, secured within edge welded stainless steel brackets, with a vented C-section beam on top, Fig. 1. Here, the x-y-z coordinate system defines orientation for all indentation cases. Experimental section photographs were recorded using a LG (Seoul, South Korea) Reflect™ (L555DL) cell phone with 13 MP digital camera. Parameters for the module are: Dimensions of 280 x 180 x 150 mm; mass of 13.2 kg; nominal voltage of 21 V; rated capacity of 63 Ah; watt-hour rating of 236.25 Wh [10]. Prior to indenting, modules were slowly discharged to a very low SOC (less than 1 V) using an electrical resistive heating element immersed in ambient tap water. After discharging, voltage gradually increased to a higher level of about 10 V at the beginning of indention tests. However, the batteries were much safer to indent because most of their energy had been dissipated.

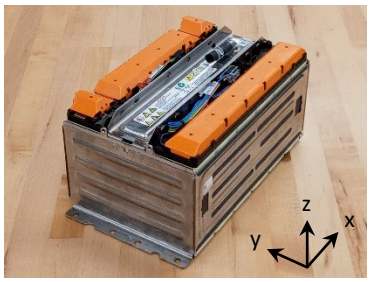

Fig. 1 Prismatic cell LIB module with x-y-z coordinate system.

Figure 2 shows the experimental setup where a V-shaped stainless steel wedge [7] was used to indent the battery modules using an Instron (Norwood, MA) 8802 servohydraulic test system. A 150 mm DIA bottom compression platen was used to support thick Al alloy 6061 module base plate(s). The wedge was attached by gripping its threaded rod connector. The actuator speed was 0.05 mm/s (quasi-static tests) or 50 mm/s (single higher rate test) and the force-displacement sampling rate was 0.125 kS/s. A Tektronix (Beaverton, OR) TBS 2102 Digital Oscilloscope recorded battery module voltage at 0.125 kS/s (same as the Instron 8802 rate for convenient file merging) during indentation. 3500 K LED light sources which matched room lighting and camera white balance settings were mounted to tripods for enhanced lighting. Most digital photographs were recorded using a tripod mounted 32.5 Megapixel Canon (Tokyo, Japan) 90D digital camera with Canon EF-S 18-135 mm f/3.5-5.6 IS USM DSLR zoom lens. These began at 0 mm and continued every 10 mm of actuator displacement up to the maximum actuator displacement of 100 mm owing to test machine range limit or test end if earlier. 120 FPS slow motion video at Full HD (1080p) recorded the higher rate case. Indentations were performed for six different orthogonal directions at the lower quasi-static speed with manual oscilloscope triggering. For the single higher rate test, channel 1 of the digital oscilloscope recorded battery module voltage while channel 2 was used for quick triggering. The 10-mV threshold trigger signal was initiated by dynamic motion of a PCB Piezotronics (Depew, NY) model 353B03 quartz shear ICP® accelerometer hot glued to the lower grip of the test machine and connected to a model 482C15 ICP® sensor signal conditioner.

Fig. 2 Experimental setup for LIB module indentation tests.

IV. Results and Observations

A. Case 1 (x parallel to z)

Figure 3 shows the force-displacement-voltage responses, where displacement represents actuator displacement. Here, x parallel to z indicates indentation along the x direction with wedge edge parallel to the z direction. All indentation cases follow this orientation convention. Figure 4 shows photographs of the battery module before and at maximum wedge indentation. Table. 1 lists observations. All case events are listed in chronological order.

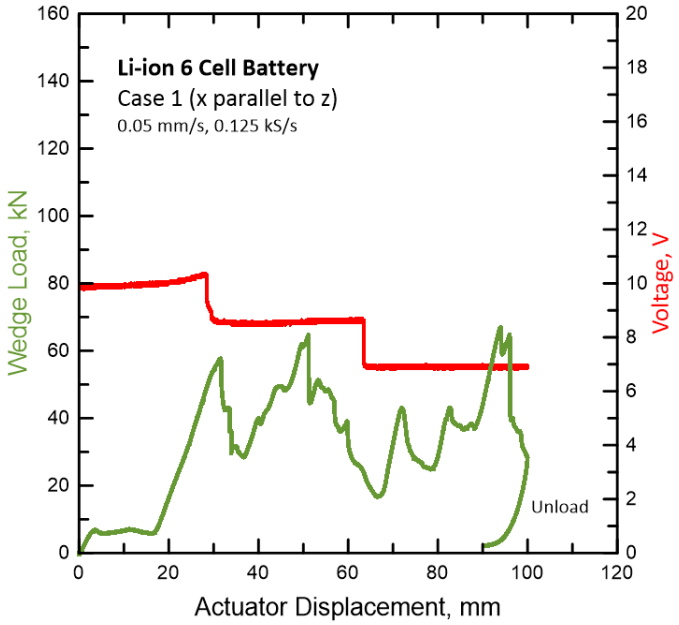

Fig. 3 Force-displacement-voltage responses for Case 1.

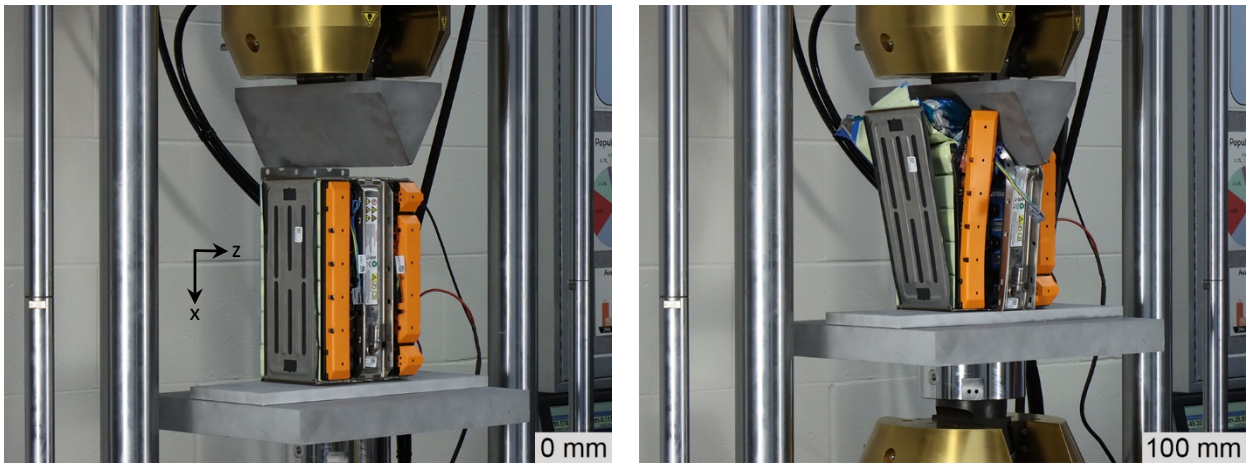

Fig. 4 Photographs before (left) and at maximum (right) wedge indentation for Case 1.

Table. 1 Wedge indentation observations for Case 1.

Event	Displacement (mm)	Force (kN)	Observation
First voltage drop	28	49	Wedge penetrates first cell
First force spike	32	57	Side steel weld edge breaks
Second force spike	51	65	Top C-section beam begins to bend
Second voltage drop	64	24	Wedge penetrates second cell
Final force spike(s)	94	67	Top C-section beam severely bent

B. Case 2 (x parallel to y)

Figure 5 shows the force-displacement-voltage responses. Figure 6 shows photographs of the battery module before, during, and after wedge indentation. The maximum actuator displacement for this case was ~45 mm due to ejection of the cells. Table. 2 lists observations.

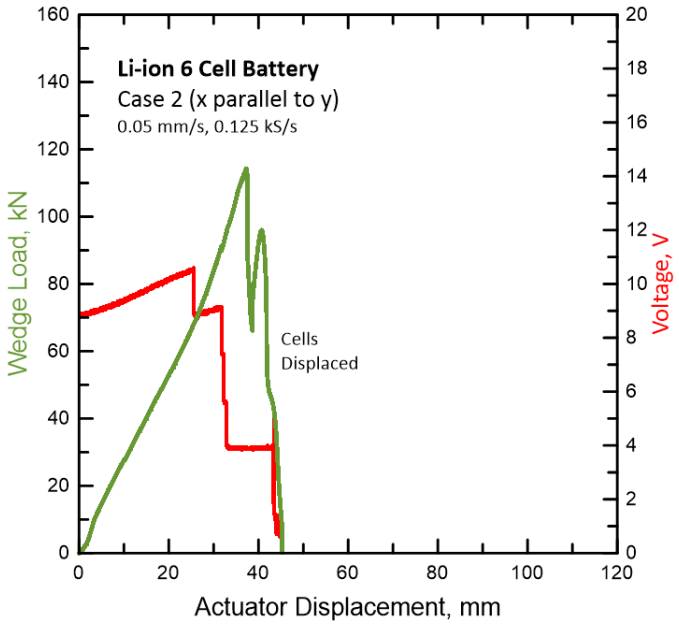

Fig. 5 Force-displacement-voltage responses for Case 2.

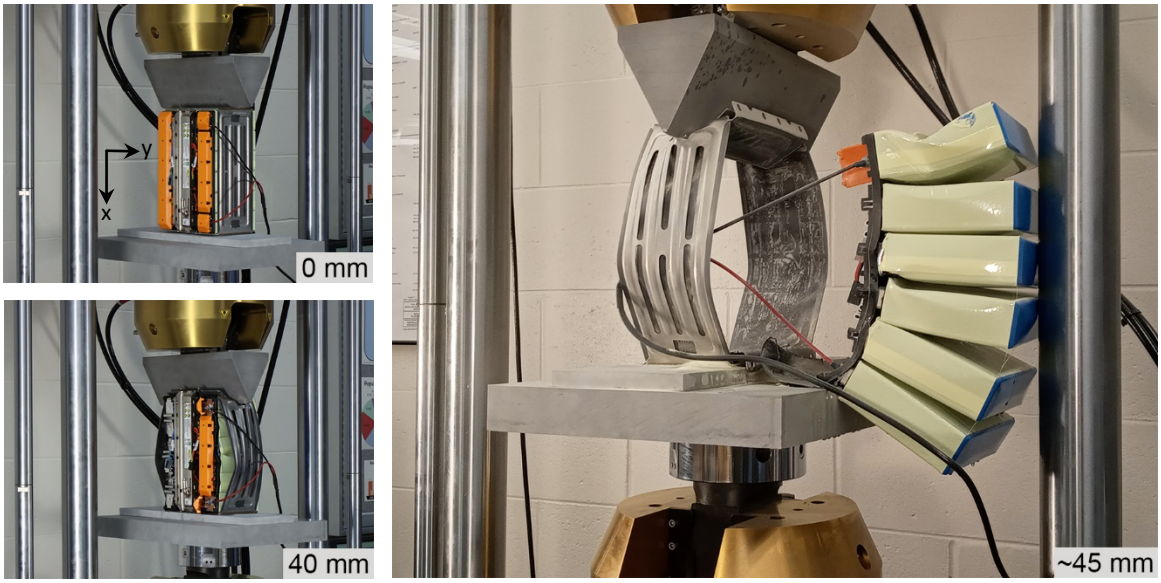

Fig. 6 Photographs before/during (left) and at maximum (right) wedge indentation for Case 2.

Table. 2 Wedge indentation observations for Case 2.

Event	Displacement (mm)	Force (kN)	Observation
First voltage drop	26	68	Wedge damages first cell
Second voltage drop	32	90	Damage continuing
First force spike	37	114	Side steel buckled
Second force spike	41	96	Middle cells cracking
Third voltage drop	43	44	Middle cells broken, then ejected

C. Case 3 (y parallel to x)

Figure 7 shows the force-displacement-voltage responses. Figure 8 shows photographs of the battery module before, during, and after wedge indentation. Owing to page limits, this is the only case where photographs are shown every 10 mm, grouped on their own page for continuity and clarity. Table. 3 lists observations.

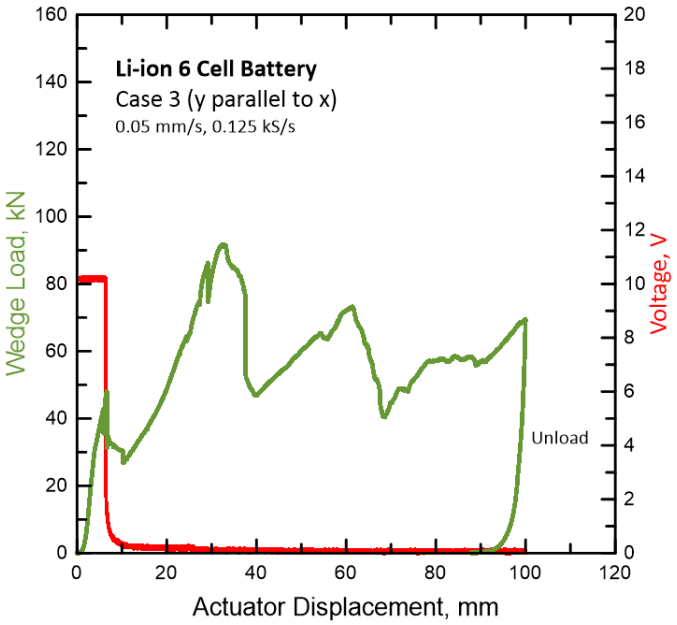

Fig. 7 Force-displacement-voltage responses for Case 3.

Table. 3 Wedge indentation observations for Case 3.

Event	Displacement (mm)	Force (kN)	Observation
First voltage drop	6	46	Side steel deformed
First force spike	7	48	Side steel deformed
Second force spike(s)	33	92	Side steel ejected
Third force spike	61	73	End cells expelled

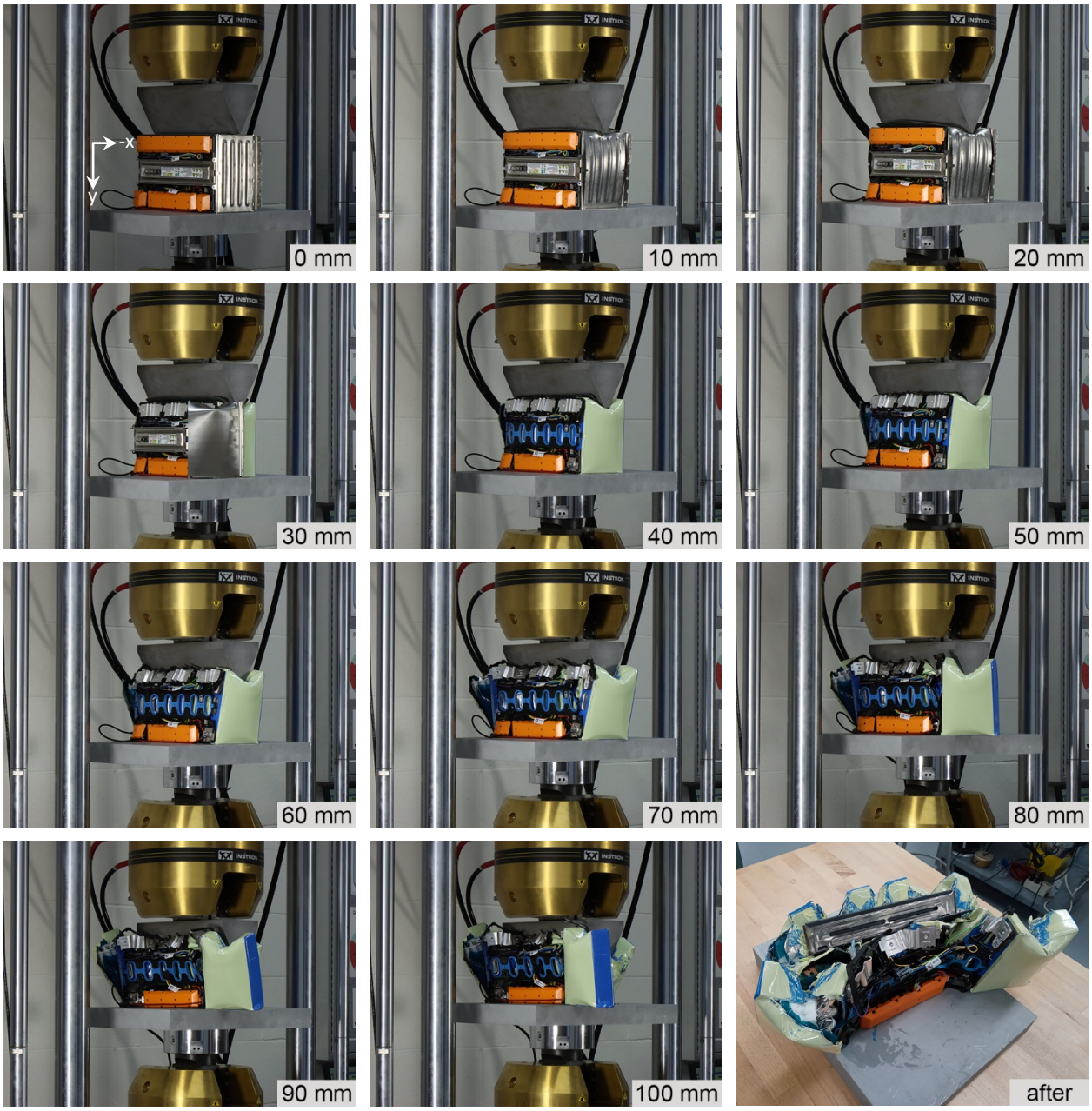

Fig. 8 Photographs before, during, and after wedge indentation for Case 3.

D. Case 4 (-z parallel to x)

Figure 9 shows the force-displacement-voltage responses. Figure 10 shows photographs of the battery module before and near maximum wedge indentation. The maximum actuator displacement for this case was ~52 mm due to machine unload at the loadcell limit (250 kN). Table. 4 lists observations.

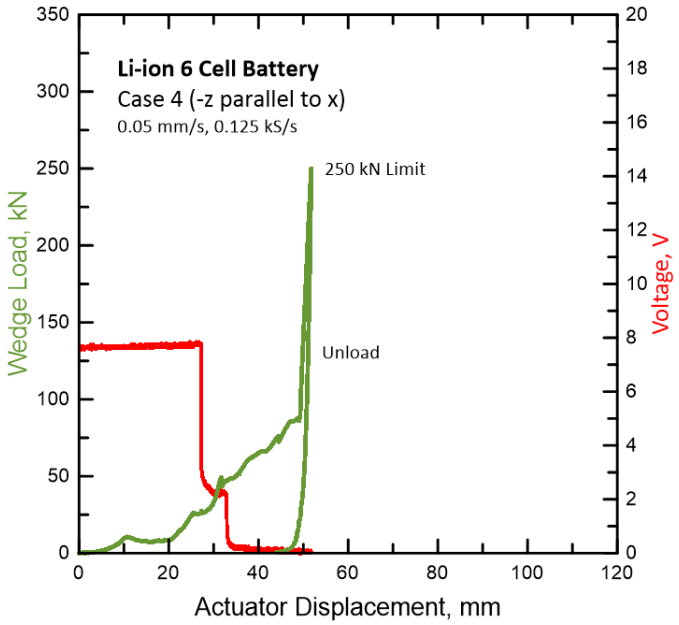

Fig. 9 Force-displacement-voltage responses for Case 4.

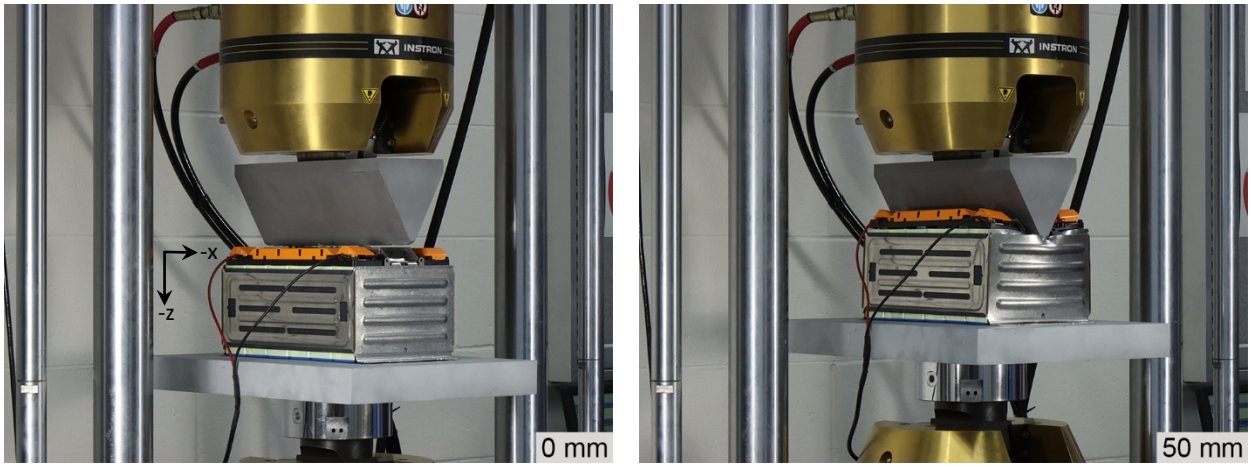

Fig. 10 Photographs before (left) and near maximum (right) wedge indentation for Case 4.

Table. 4 Wedge indentation observations for Case 4.

Event	Displacement (mm)	Force (kN)	Observation
First voltage drop	27	26	Top C-section beam deformed
Second voltage drop	33	47	Wedge first strikes side steel
Force spike	52	250	Side steel deformed

E. Case 5 (y parallel to z)

Figure 11 shows the force-displacement-voltage responses. Figure 12 shows photographs of the battery module before and at maximum wedge indentation. Table. 5 lists observations.

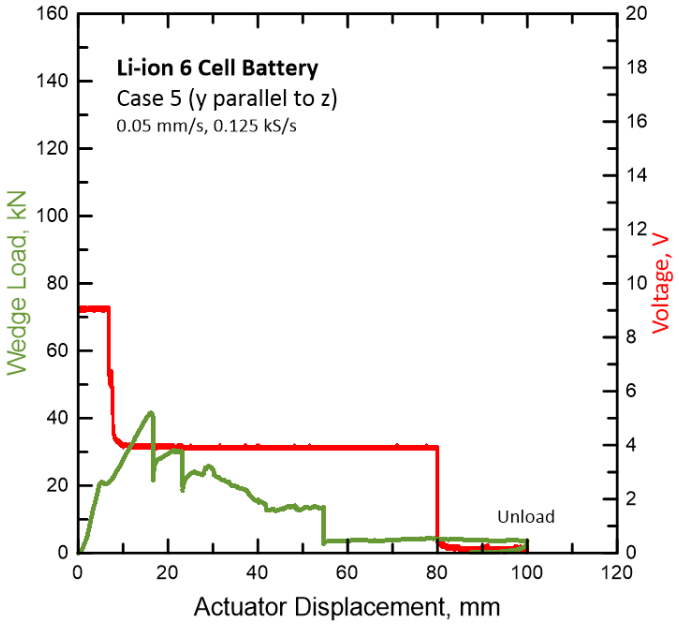

Fig. 11 Force-displacement-voltage responses for Case 5.

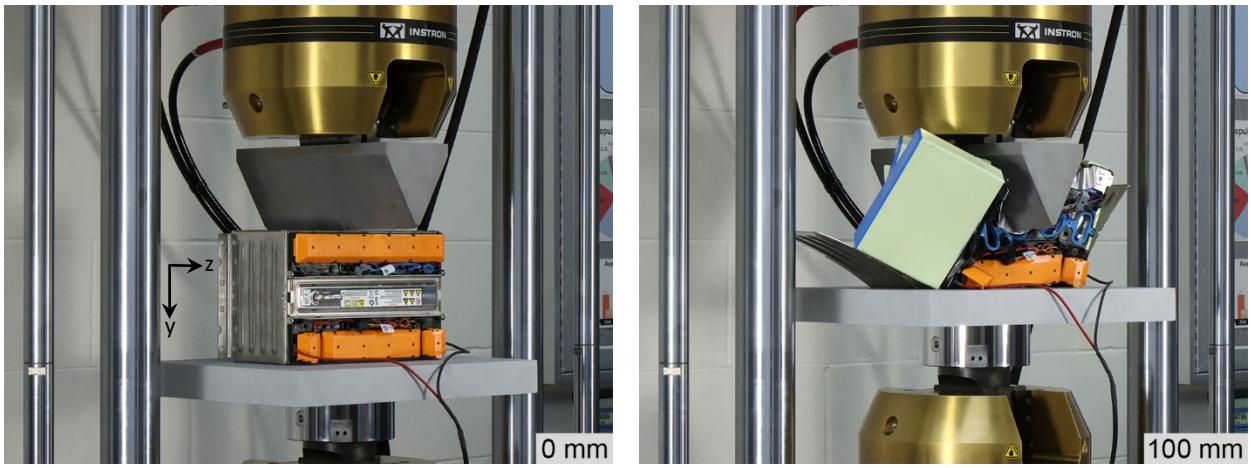

Fig. 12 Photographs before (left) and at maximum (right) wedge indentation for Case 5.

Table. 5 Wedge indentation observations for Case 5.

Event	Displacement (mm)	Force (kN)	Observation
First voltage drop	7	21	Wedge bends side steel
First force spike	16	41	First side steel weld edge breaks
Second force spike	23	30	Second side steel weld edge breaks
Force drop	55	14	C-section beam ejected
Second voltage drop	80	4	Cells expelled

F. Case 6 (-z parallel to y)

Figure 13 shows the force-displacement-voltage responses. Figure 14 shows photographs of the battery module before and at maximum wedge indentation. Table. 6 lists observations.

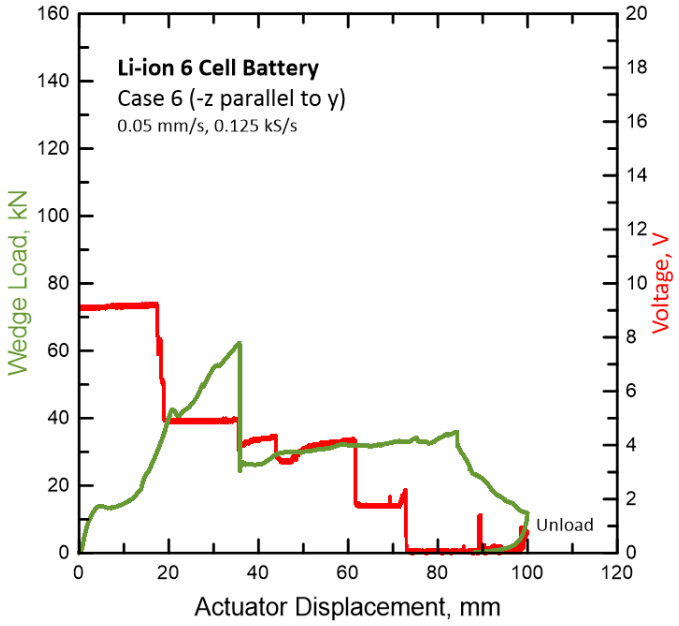

Fig. 13 Force-displacement-voltage responses for Case 6.

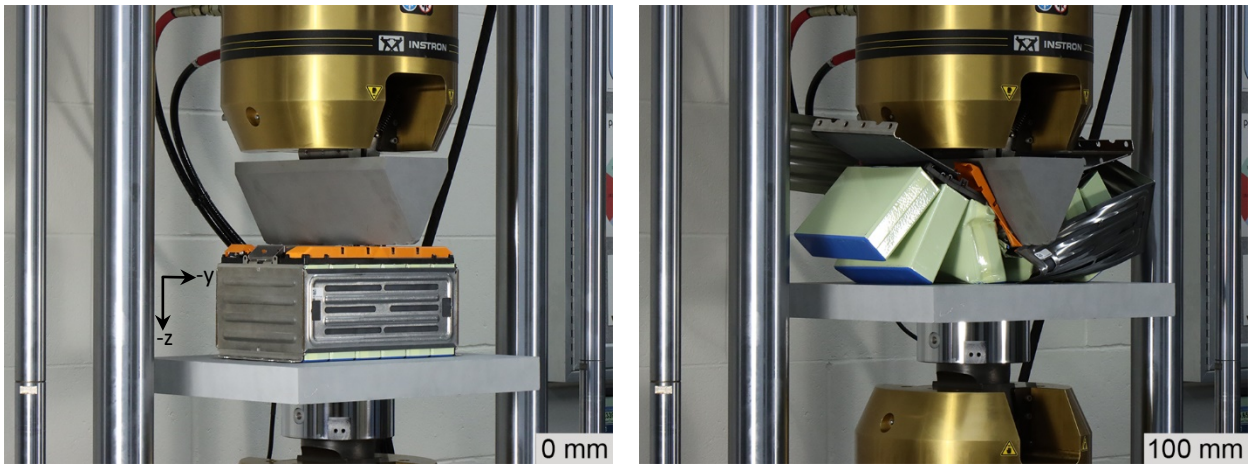

Fig. 14 Photographs before (left) and at maximum (right) wedge indentation for Case 6.

Table. 6 Wedge indentation observations for Case 6.

Event	Displacement (mm)	Force (kN)	Observation
First voltage drop	18	31	Wedge deforms top C-section beam
First force spike	36	62	Side steel breaks off
Remainder	36 - 100	16 - 32	Damage continuing and cells expelled

G. Case 7 (x parallel to z)

This loading orientation was the same as Case 1 but occurred at a rate of 50 mm/s rather than 0.05 mm/s. Figure 15 (left) shows the force-displacement-voltage responses. The battery and trigger voltage-time responses are shown in Fig. 15 (right); loading was too fast for manual triggering. Figure 16 shows photographs of the battery module before and at maximum wedge indentation as recorded by slow motion video. Table. 7 lists approximate observations based on slow motion video footage of the higher speed event.

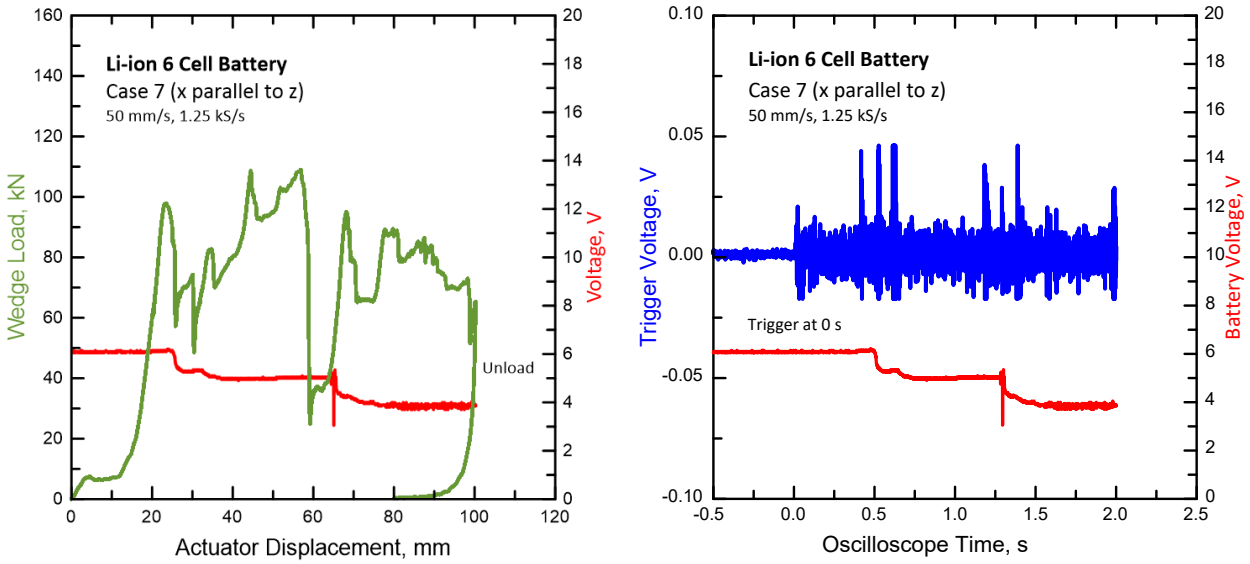

Fig. 15 Force-displacement-voltage responses (left) and triggering response (right) for Case 7.

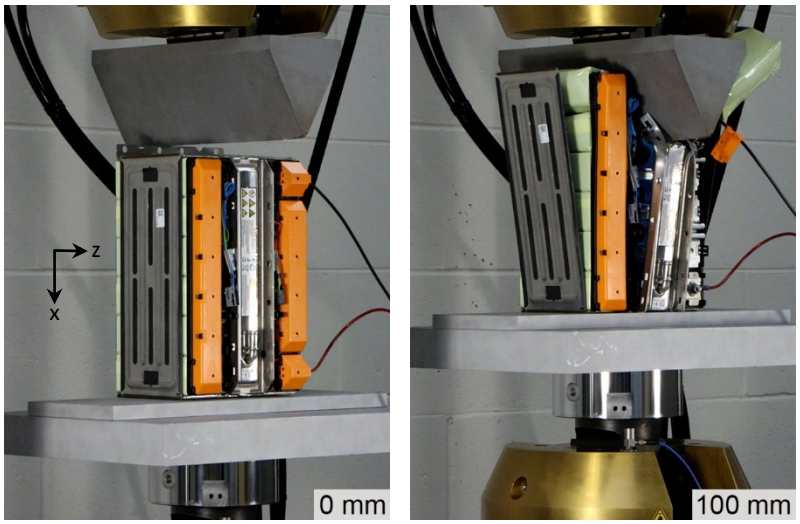

Fig. 16 Photographs before (left) and at maximum (right) wedge indentation for Case 7.

Table. 7 Wedge indentation observations for Case 7.

Event	Displacement (mm)	Force (kN)	Observation
First force spike	~22	~97	One side steel weld edge breaks
First voltage drop	~25	~85	Wedge penetrates first cell
Force drop	~30	~73	Both side steel weld edges break
Force spike	~70	~79	Top C-section beam severely bent

V. Conclusion

Discharging the battery modules to very low SOC was necessary for test safety. After discharging, voltage gradually increased to a higher level, but most of their energy had been dissipated. While measuring force and voltage as a function of displacement, progression of damage of the cells within the battery modules was photographed and observed. Results differed substantially depending on loading orientation and direction. A few notable observations follow. The lowest peak forces were 41 kN and 62 kN for Case 5 and Case 6 respectfully, where the V-shaped wedge indented between the central cells. Here, Case 6 had a higher initial peak force than Case 5 which is likely due to the extra force resistance afforded by the top C-section beam whereas Case 5 only had a single thin steel plate to resist the initial loading. Case 4 had the highest force for all 7 cases, exceeding the loadcell limit. Here, the wedge indented the top C-section beam, all cells, two side steels, while all edge welds remained intact, leading to the highest force resistance amongst all cases. In other cases, load dropped soon after breakage of the side steel weld(s). In most cases, cells were partially or fully expelled. For example, ejection of the cells for Case 2 occurred through the module base where there was no support structure to constrain them. The largest single voltage drop occurred for Case 3. Here, the cells were nearly simultaneously loaded as there was no C-section beam, wires, etc., to resist force other than the side steel. Most other voltage drops were linked to cell damage in varying ways. For the cases with the same loading orientation but different loading rates, Cases 1 and 7, indentation forces were greater at the higher rate, however, voltage responses were similar. This force-voltage-displacement responses and visual damage observations can help engineers expand their knowledge on the effects of various loading to high-voltage LIB modules.

Acknowledgments

This work was funded by Ford Motor Company through a University Research Program project. We are grateful to J. Deng (PI), C. Bae, and S. Kim at Ford as well as F. Zhu (PI), R. Zhou, and K.P. Logakannan at Johns Hopkins University for their support and collaboration. We also wish to thank the National Science Foundation for the Instron servohydraulic test system and Embry-Riddle Aeronautical University for numerous small equipment and supplies. Professor Sypeck acknowledges assistance from students S. Xu (co-author), B. de Bruns, O. Ajimobi, C. Wells, C. Huettner, X. Wang, M. Chotoo, A. Chika, K. Maurer, A. Patil, and F. Stephen.

References

[1] Clark, P. by A., "Update: True blue TB44 Li-Ion Battery FAA certified for Caravan, Dash-8," *Disciples of Flight* [online journal], URL: https://disciplesofflight.com/lithium-ion-aircraft-battery-certified/ [retrieved 24 February 2023].

[2] Hayward, J., "A look at the battery issues that grounded the Boeing 787 in 2013," *Simple Flying* [online journal], URL: https://simpleflying.com/boeing-787-battery-issues/ [retrieved 24 February 2023].

[3] FAA, "FAA Awards Another $20.4M to Electrify Airport Equipment, Latest in $300M Investment This Year," *Federal Aviation Administration* [online database], URL: https://www.faa.gov/newsroom/faa-awards-another-204m-electrify-airport-equipment-latest-300m-investment-year.

[4] Kuta, S., "Electric Planes Are Taking Flight," *Smithsonian* [online journal], URL: https://www.smithsonianmag.com/smart-news/electric-planes-are-taking-flight-180980821/ [retrieved 24 February 2023].

[5] Xia, Y., Chen, G., Zhou, Q., Shi, X., and Shi, F., "Failure behaviours of 100% SOC lithium-ion battery modules under different impact loading conditions," *Engineering Failure Analysis*, vol. 82, 2017, pp. 149–160. doi: 10.1016/j.engfailanal.2017.09.003

[6] Kalnaus, S., Wang, H., Watkins, T. R., Simunovic, S., and Sengupta, A., "Features of mechanical behavior of EV battery modules under high deformation rate," *Extreme Mechanics Letters*, vol. 32, 2019, p. 100550. doi: 10.1016/j.eml.2019.100550

[7] Zhu, F., Lei, J., Du, X., Currier, P., Gbaguidi, A., and Sypeck, D., "Crushing behavior of Vehicle Battery Pouch Cell and module: A combined experimental and theoretical study," *SAE International Journal of Materials and Manufacturing*, vol. 11, 2018, pp. 341–348. doi: 10.4271/2018-01-1446

[8] Zhu, F., Zhou, R., Sypeck, D., Deng, J., and Bae, C., "Failure behavior of prismatic Li-ion battery cells under abuse loading condition - a combined experimental and computational study," *Journal of Energy Storage*, vol. 48, 2022, p. 103969. doi: 10.1016/j.est.2022.103969

[9] Logakannan, K. P., Zhu, F., Sypeck, D., Xu, S., Deng, J., and Kim, S., "Testing and modeling of vehicle li-ion battery module with prismatic cells under abuse conditions," *Energies*, vol. 16, 2023, p. 1055. doi: 10.3390/en16031055

[10] Lima, P., "What the future holds for the Fiat 500e?," *PushEVs - Push Electric Vehicles Forward* [online journal], URL: https://pushevs.com/2017/03/06/future-holds-fiat-500e/ [retrieved 24 February 2023].